A novel feeding mechanism of diplodocid sauropods revealed in an Apatosaurine skull from the Upper Jurassic Nail Quarry (Morrison Formation) at Como Bluff, Wyoming, USA

Joseph E. Peterson, David Lovelace, Melissa Connely, and Julia B. McHugh

ABSTRACT

Dental complexes of sauropod dinosaurs have been studied in members of Diplodocoidea and Macronaria. However, the disparity among the number of replacement teeth between the premaxilla, maxilla, and dentary of apatosaurine sauropods has yet to be fully investigated. TATE-099, a nearly complete and associated apatosaurine skull and dental complexes from the upper Morrison Formation (Upper Jurassic) at Como Bluff, Wyoming, contains cranial characters consistent with *Apatosaurus* sp. Unerupted dental complexes of the right premaxilla, maxilla, and dentary were imaged and digitally reconstructed using computed tomography (CT). Results indicate four premaxillary alveolar positions each with 5–7 unerupted replacement teeth, 10 maxillary alveolar positions each with 3–5 unerupted replacement teeth, and 10 dentary alveolar positions each with only 1–2 unerupted replacement teeth. The capacity of replacement teeth in TATE-099 is higher than reported in the genus *Diplodocus* and consistent with data from previous studies on niche partitioning among coeval Morrison Formation sauropods. Disparity among the capacity of dental complexes of TATE-099 further suggests novel feeding mechanics in apatosaurines. CT data also support a new hypothesis of tooth replacement in diplodocids, where entire rows of teeth are replaced as a single unit, rather than individually. The high-capacity of replacement teeth in the premaxilla is only known to be succeeded by one taxon (*Nigersaurus*) and suggests frequent wear of the premaxillary teeth. However, considerably fewer replacement teeth in the dentary of TATE-099 suggests less-frequent. These results offer insight into the feeding mechanisms and disparity of sauropods within Flagellicaudata.

Joseph E. Peterson. University of Wisconsin-Oshkosh, Department of Geology, 800 Algoma Boulevard, Oshkosh, Wisconsin 54901, USA. petersoj@uwosh.edu (corresponding author)
David Lovelace. University of Wisconsin-Madison, Geology Museum, Madison Wisconsin 53706, USA. dlovelace@wisc.edu

Melissa Connely. Stratigraphic rex LLC, Casper, Wyoming 82604, USA. melconn45@gmail.com
Julia B. McHugh. Museums of Western Colorado, Grand Junction, Colorado, 81502, USA and Colorado Mesa University, Department of Physical and Environmental Sciences, Grand Junction, Colorado, 81502, USA. jmchugh@westcomuseum.org

---

INTRODUCTION

Sauropod dinosaurs are the largest land animals the Earth has ever seen. These gigantic herbivores had a deep impact on the local environments and ecosystems they inhabited. Moreover, rapid rates of growth (e.g., Curry, 1999; Lehman and Woodward, 2008; Sander et al., 2011) and unique morphologies often linked to specific niches and novel modes of food procurement (e.g., Christian et al., 2013; Hummel et al., 2008; Stevens and Parrish, 2005; Whitlock, 2011) may have driven their success as ecological titans. Dental complexes of sauropod dinosaurs have been studied in Diplodocidae, Rebbachisauridae, and Camarasauridae (D'Emic et al., 2013; Schwarz et al., 2015; Sereno et al., 2005; Stevens and Parrish, 2005) demonstrating that dental morphology and physiology (i.e., tooth and alveolar arrangement and tooth replacement strategies) directly impact feeding, digestion, and even food procurement. As such, these dental systems can provide considerable insight into sauropod paleobiology and paleoecology (e.g., Barrett and Upchurch, 1995; Fiorillo, 1998; Gee, 2011; McHugh, 2018; Tütken, 2011).

Sauropod remains are found within Cretaceous and Jurassic deposits throughout the world. In North America, the rich sauropod fossil record from the Upper Jurassic Morrison Formation has the potential to yield a robust understanding of coeval sauropod taxa with a global distribution as well as endemic taxa like *Apatosaurus* and *Brontosaurus* (e.g., Foster and Peterson, 2015; Hummel et al., 2008; McHugh, 2018; Rees et al., 2004; Tschopp et al., 2015, 2022).

Dietary habits and adaptations in sauropods have dominantly been studied through the lenses of rates of tooth replacement, neck biomechanics, tooth microwear, snout shapes, species richness, and estimates of population densities (e.g., Barrett and Upchurch, 1995; D'Emic et al., 2013; Fiorillo, 1998; Gee, 2011; McHugh, 2018; Schwarz et al., 2015; Sereno et al., 2005; Stevens and Parrish, 2005; Tütken, 2011; Whitlock, 2011; Whitlock et al., 2018). These studies reveal a wide range of diet-linked morphologies among different taxa; however, variance in the number of replacement teeth observed in the premaxilla, maxilla, and dentary among apatosaurine sauropods has yet to be fully investigated. It may be premature to compare intergeneric differences before first understanding intraspecific disparity of tooth replacement strategies. Here, we describe a nearly complete and associated *Apatosaurus* skull (TATE-099) collected from the upper Morrison Formation in Wyoming and examine the preserved dental apparatuses to shed further light on the paleoecology of the genus.

Geological Setting

The Morrison depositional basin captured Late Jurassic sediments throughout much of the Rocky Mountain west, preserving a record that spans ca. 156–148 Ma (see Maidment and Muxworthy, 2019) (Figure 1A). It has been demonstrated that there is a time-transgressive nature to Morrison deposition where the southern half of the depositional basin exhibits thick, well-defined stratigraphic successions that can be broken into discrete members. However, the formation youngs north of the Colorado Plateau (i.e., Wyoming, Montana, South Dakota) where local-scale divisions have been proposed (i.e., Allen, 1996; Bakker, 1996); more typically, exposures north of the plateau are considered 'undivided' (e.g., Foster, 2020; McMullen, 2017). Lithostratigraphic correlations between Como Bluff and units on the Colorado Plateau remain tenuous, although detrital radioisotopic dates have been used to constrain maximum depositional ages enabling chronostratigraphic correlation with time-equivalent units across the Morrison Basin (e.g., Trujillo et al., 2014; Maidment and Muxworthy, 2019 and references therein; Whitlock et al., 2018).

Stratigraphy and Taphonomy

TATE-099 was discovered in 1996 at Nail Quarry (Connely, 2002; Foster, 2003), Como Bluff, WY. The quarry is positioned roughly halfway up the formation in a grey/green illitic mudstone (Fig-
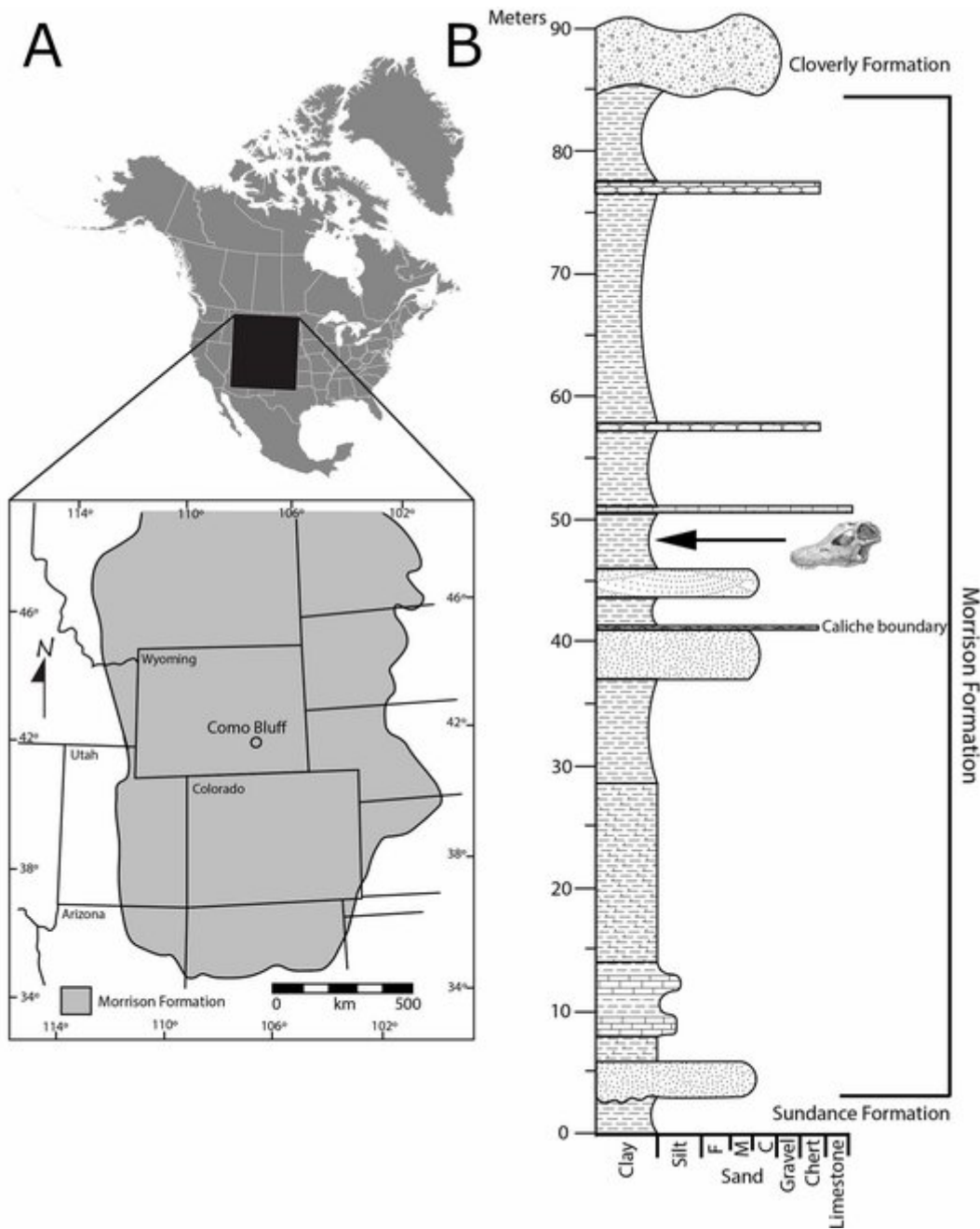
FIGURE 1. A. Depositional area of the Upper Jurassic Morrison Formation, and location of the Nail Quarry in southeastern Wyoming, and B. the stratigraphic location of Nail Quarry in the Morrison Formation.

ure 1B) immediately above the pedogenic calcite-rich 'boundary caliche' (sensu Allen, 1996). The 'boundary caliche' is considered to be a time-surface and has been used as a datum for local correlations (Allen, 1996; Bakker, 1996; Connely, 2002); it is also the contact between the locally defined 'Lake Como' and the 'Talking Rocks' members (*sensu* Allen, 1996; Bakker, 1996). Although these two units were promoted by Allen (1996), their use has not been adopted by the majority of Morrison Fm. workers. For instance, rather than using 'Talking Rocks', Connely (2002) describes

this interval as Unit B, with Nail quarry being at the very base. Connely suggests that unit boundaries are characterized by a change in sediment source (e.g., a higher concentration of volcaniclastic input) rather than a change in climate, as both Unit B and the underlying Unit A exhibit sedimentary features consistent with strong seasonality, in line with observations in Morrison Formation in Bighorn Basin, WY (Jennings and Hasiotis, 2006).

The Nail Quarry bone bed is approximately 2 m thick with an excavated area of ca. 10 x 7 m; the full extent of the still-active quarry remains unknown. Excavated specimens are largely disarticulated elements of adult animals, although many specimens do show some signs of association (Connely, 2002). TATE-099 is one of a small percentage of specimens retaining some degree of articulation and strong association. Many of the elements in the quarry exhibit abundant bite marks that, according to some (Bakker et al., 1997; Connely, 2002; Bakker and Bir, 2004), are attributable to *Allosaurus* based on the high quantity of shed teeth. It has been hypothesized that *Allosaurus* was the dominant, if not only, carnivore responsible for the traces at Nail Quarry (Bakker et al., 1997). Other observations of high concentrations of theropod bite traces within the Morrison depositional basin are not unusual, though most are not restricted to only *Allosaurus* (i.e., Drumheller et al., 2020; Jennings and Hasiotis, 2006).

Specimen History

TATE-099 is a sub-articulated/associated apatosaurine skull collected from Nail Quarry at Como Bluff, Wyoming in 1996 by the Dinamation International Society of Colorado. Elements included the entire skull, both lower jaws, and a complete set of maxillary teeth separated from the skull but still in direct association to each other. The skull was also articulated with the first four cervical vertebrae and closely associated with cervicals 5 and 6. The first four cervicals were, unfortunately, crushed under the weight of an overlying sacrum and ilium of a large sauropod at the quarry; however, the axis remained fairly intact. The atlas and axis were removed from the jacket containing the pelvis and prepared, but C3 and C4 remain unprepared in the now resealed field jacket at the Tate Geological Museum (TATE), Casper College, Casper, WY. The jacket containing cervicals 5 and 6 was vandalized in the field; salvaged material is currently unprepared in collections at the Paleon Museum, Glenrock, WY.

The skull elements recovered from the field in the Fall of 1996 were prepared by the staff and volunteers at the Tate Geological Museum. The specimen was molded using a silicone molding compound. A wax cast was made using microcrystalline sculpting wax with a low shrinkage rate. The wax casts were then manipulated into the original bone shape and damaged areas were reconstructed. The casts were then remolded to provide a complete skull for display and study (Connely and Hawley, 1998).

Shortly thereafter, the skull, axis, and atlas were borrowed for scientific illustration and CT imaging for additional research and publication; it is unknown if these scans were ever conducted. The specimen was not returned, and the loan remained outstanding until 2015 when the maxillae, premaxillae, dentary, and a number of small cranial elements were brought to the Denver Museum of Nature and Science vertebrate paleontology collections (DMNH EPV) and then transferred back to the Tate Geological Museum. However, the original braincase, atlas/axis, and several other unprepared elements were not part of this transfer and return and remain unavailable for study.

Computed Tomography and 3D Printing

In order to fully explore the oral apparatus, the unerupted dental complexes in the right premaxilla, maxilla, and dentary of specimen TATE-099 were imaged and reconstructed using computed tomography (CT), then digitally segmented and exported as stereolithograph models (STL) for analysis.

Since no known X-ray data exists from previous workers' attempts to scan the specimen, CT scans were taken at the Wyoming Medical Center (Casper, WY), and the St. Anthony Medical Center with an Aquilion Toshiba 64-slice CT scanner conducted at settings for medical diagnoses of bone pathology (135 kV, 300 mA, 0.5 mm pixel resolution, and 0.6 mm thickness). Analysis of CT data was conducted in Object Research Systems Dragonfly software (a free license is available for academics; Dragonfly, 2020.2). 3D Slicer was used to manually segment and isolate each tooth from the surrounding matrix. The resultant 3D models were transferred to the free program Meshmixer (Autodesk, version 3.5) where the meshes were refined and the excess background matrix was deleted. Support cylinders were also added where needed to connect 'free-floating' teeth. After digital stabilization, the models were exported as stereolithography (STL) files (Supplementary Figure files

S1-S12). The 'Make Solid' algorithm was utilized to prepare the STL models for printing by filling 'gaps' in the model meshes as well as the removal of artifacts from the scanning process. The solid mesh models were then imported into UP Studio (version 0.0.10) for rapid prototyping on an UP Mini 3D printer. All prints were made with 1.75 mm white Octave acrylonitrile butadiene styrene (ABS) filament and printed in 200 μm layers.

Institutional Abbreviations. AMNH, American Museum of Natural History; **CM,** Carnegie Museum of Natural History; **CMC VP,** Cincinnati Museum of Natural History and Science; **DMNH EPV,** Denver Museum of Nature and Science; **HMNS,** Houston Museum of Nature and Science; **MNN,** Musee National du Niger; **MWC,** Museums of Western Colorado; **SMA,** Sauriermuseum Aathal; **TATE,** Tate Geological Museum; **USNM,** National Museum of Natural History, Smithsonian Institution. **YPM,** Yale Peabody Museum; **LACM,** Los Angeles County Museum; ML, Museu da Lourinhã; **MB.R,** Museum für Naturkunde; **MCNV,** Museo de Ciencias Naturales

SYSTEMATIC PALEONTOLOGY

SAURISCHIA Seeley, 1887
SAUROPODOMORPHA Huene, 1932
SAUROPODA Marsh, 1878
DIPLODOCIDAE Marsh, 1884
APATOSAURINAE Janensch, 1929
APATOSAURUS Marsh, 1877
APATOSAURUS sp.

Diagnosis. TATE-099 possesses a widely diverging basipterygoid process greater than 60º (Wilson, 2002), and lacks the basisphenoid/basipterygoid recess (Tschopp et al., 2015). These character states are consistent with the genus *Apatosaurus*.

Material. The currently observable elements of TATE-099 include: left and right premaxillae, maxillae, and ectopterygoids; left quadratojugal, quadrate, palatine, and pterygoid; right dentary and partial right surangular and angular (Figures 2-9). The braincase is represented by a plastic replica (with some apparent reconstruction); the whereabouts of the original, along with the first four cervical vertebrae (at minimum) are currently unknown.

Locality. Nail Quarry, Como Bluff, Wyoming.

Horizon. C5/C6 system tract (sensu Maidment and Muxworthy, 2019).

Age. Late Kimmeridgian to early Tithonian (Maidment and Muxworthy, 2019).

DESCRIPTION

We use traditional anatomical orientational descriptors and terminology in the descriptions below following Tschopp et al. (2015).

Dermal Roof Complex

Both premaxillae of TATE-099 are present (Figure 2A-D). The premaxillae are long, slender tooth-bearing elements that laterally contact the maxillae and medially contact each other, and posteriorly terminating at the external nares. Each premaxilla measures 295 mm in total assembled length and 80 mm in maximum height of the symphysis at the body.

The posterior-most 80 mm of the nasal processes of both premaxillae are separated and are adhered to the ventral side of the right maxilla. The right premaxilla is fractured and displaced dorsally across the lateral alveolar process. Four alveolar positions are present in each premaxilla.

The shape of the anterior margin of the premaxilla lacks a step and the external surface lacks anteroventrally-oriented vascular grooves. In dorsal view, the main body and elongate ascending nasal process are a single unit without an obvious distinction between regions, and the angle between the lateral and medial margins of the premaxilla is less than 17º (Tschopp et al., 2015; Upchurch, 1999).

The posteroventral edge of the ascending process (in lateral view) is straight and directed posterodorsally. The posterolateral process and the lateral process of the maxilla lacks a midline contact. The subnarial foramen and the anterior maxillary foramen are separated by a bony isthmus, as seen in CM 11161 (Tschopp et al., 2015).

Both maxillae of TATE-099 are present and exhibit slight crushing and distortion dorsoventrally (Figures 3-4). The maxillae are large, thin sheets of bone divided by the antorbital fenestra into an ascending process and a posterior process contacting the quadratojugal and jugal. The left maxilla measures 350 mm in length and 170 mm maximum width, and the right maxilla measures 330 mm in length and 165 mm maximum width. Each maxilla possesses 10 alveolar positions.

The maxillae of TATE-099 possess a concave dorsal margin of the antorbital fenestra. The anterior maxillary foramen lies on the medial edge of the maxilla, opening medially into the premaxillary-maxillary boundary. The posterior extent of the dorsal process of the maxilla extends posterior to the posterior process of the maxilla, and the maxilla-quadratojugal contact is broad.
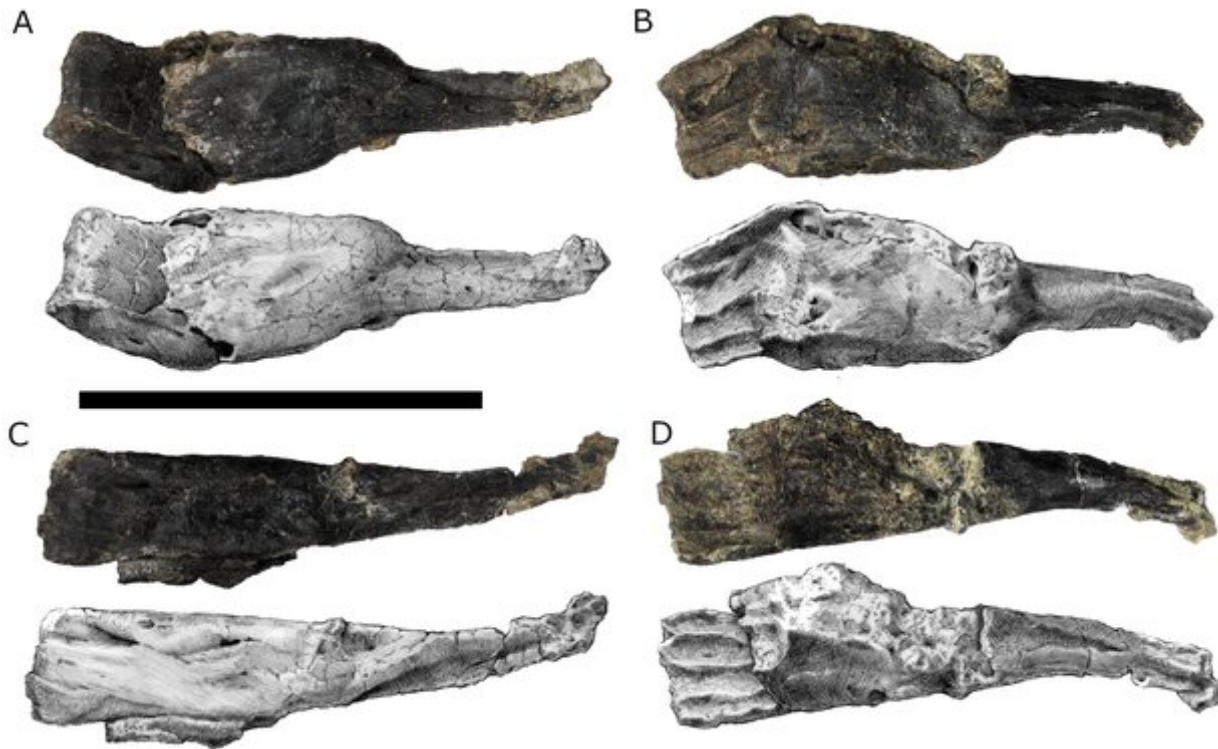
FIGURE 2. Left (A, B) and right (C, D) premaxillae in dorsal ventral views, respectively. Scale bar equals 10 cm. Artwork by Ryan Steiskal.

The preantorbital fossa is present and dorsally capped by a thin, distinct crest. This is also present in the genus *Diplodocus* and is found throughout the clade Flagellicaudata, and only absent in *A. louisae* (CM 11162). The preantorbital fenestra is present and occupies at least 50% of the preantorbital fossa. The anterior extension of the antorbital fenestra is restricted posterior to the preantorbital fossa. The narrow bony bridge that is present between the large foramen anterior to the preantorbital fossa observed in *Dicraeosaurus hansemanni* (MB.R.2336) is absent in TATE-099, as it is in diplodocids (Tschopp et al., 2015). Similarly, the foramen posterior to the antorbital maxillary foramen, and dorsal to the preantorbital fossa present in *Galeamopus pabsti* (SMA 0011; Tschopp and Mateus, 2017) is absent in TATE-099, which is a character state common in most but not all diplodocids (e.g., present in *Kaatedocus siberi* SMA 0004) (Tschopp et al., 2015).

The left quadratojugal is present and is attached to the left quadrate and left pterygoid.

The quadratojugal is dorsoventrally slender and antero-posteriorly elongate, and contacts and partially overlaps the quadrate.

The left quadratojugal (Figure 5A-B) measures 150 mm in length and the articular surface to the quadrate measures 80 mm tall. The anterior terminus of the quadratojugal extends beyond the anterior margin of the orbit. The angle between the anterior and dorsal processes of the quadratojugal is roughly 130 degrees, allowing the quadrate shaft slants posterodorsally (Tschopp and Mateus, 2013).

The full shape of the reconstructed snout (Figure 6) of the craniofacial skeleton in dorsal view has a average premaxillary-maxillary index (PMI) of 86.25%, making it more square-shaped than the average for *Galeamopus pabsti* (AMNH 969, USNM 2673) and *Diplodocus* (CM 11161, USNM 2672,) and *Apatosaurus* (CM 11162, CMC VP7180), which have a PMI of 84%, but less than *Nigersaurus* (MNN GAD 512), which has a PMI of 95% (Whitlock, 2011).

Palatal Complex

The left quadrate is present and fused with the left pterygoid (Figure 5A-B). The quadrate articulates with the dermal skull roof and the palate. The quadrate measures 173 mm in height from the base of the mandibular articular condyle to the pos-
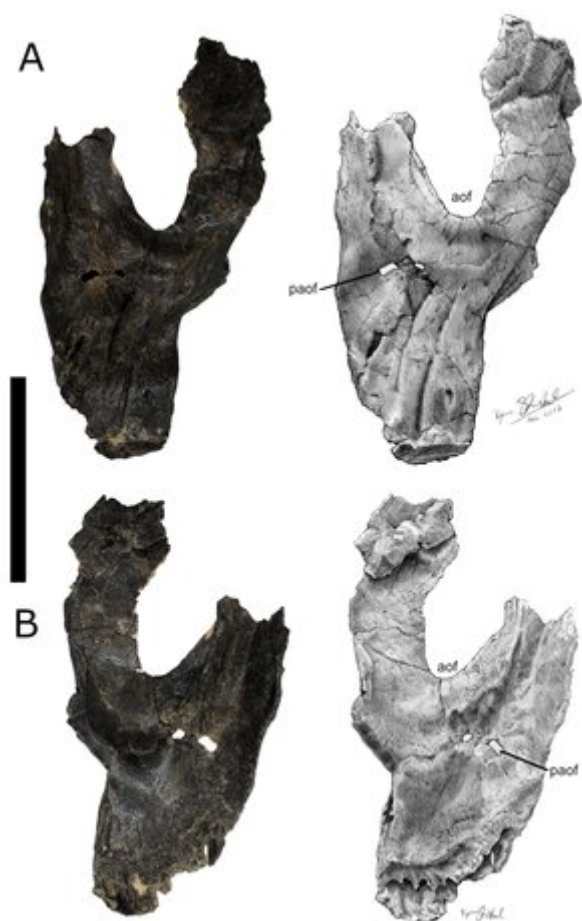
FIGURE 3. Right maxilla in (A) dorsal and (B) ventral views with the left ectopterygoid (i) and left palatine (ii) adhered to the ventral surface. Scale bar equals 10 cm. Artwork by Ryan Steiskal. Abb: aof, antorbital fenestra; paof, preantorbital fenestra.

FIGURE 4. Left maxilla in (A) dorsal and (B) ventral views. Scale bar = 10cm. Artwork by Ryan Steiskal. Abb: aof, antorbital fenestra; paof, preantorbital fenestra.

terior end of the quadrate. The articular surface of the quadrate is roughly triangular in shape. A short transverse ridge is present medially on the posterior side of the ventral ramus of the quadrate, near the articular surface with the lower jaw. The quadrate fossa is shallow and lacks a second fossa medial to the pterygoid flange on the quadrate shaft. The quadrate possesses a straight dorsal margin, providing no clear distinction with the posterior extension of the pterygoid flange, while the posterior end of the quadrate is slender and elongated.

The left pterygoid is present and fused with the left quadrate. The pterygoid measures 134 mm tall from the pterygoid process to the ectopterygoid process. The shape of the palatobasal contact of the pterygoid resembles a small facet. The transverse flange (i.e., ectopterygoid process) is positioned anterior to the antorbital fenestra.

The palatine is a thin bone widening to a spatulate-shape that articulates posteriorly and anterodorsally with the vomer in life. The left palatine is present in TATE-099 and is adhered to the ventral surface of the left maxilla, measuring 90 mm in length (Figure 4Bi).

The ectopterygoids (Figure 7) are curved elements that articulate laterally to the maxillae and palatine, and posterormedially to the pterygoids in life. Both left and right ectopterygoids are present in TATE-099. The left ectopterygoid is attached to the ventral surface of the left maxilla and measures 70 mm in length. The right ectopterygoid is disarticulated from the maxilla.

Braincase

The original specimen of the braincase of TATE-099 is currently unavailable for study. However, a reconstructed cast replica of the braincase was available and analyzed, noting areas that were
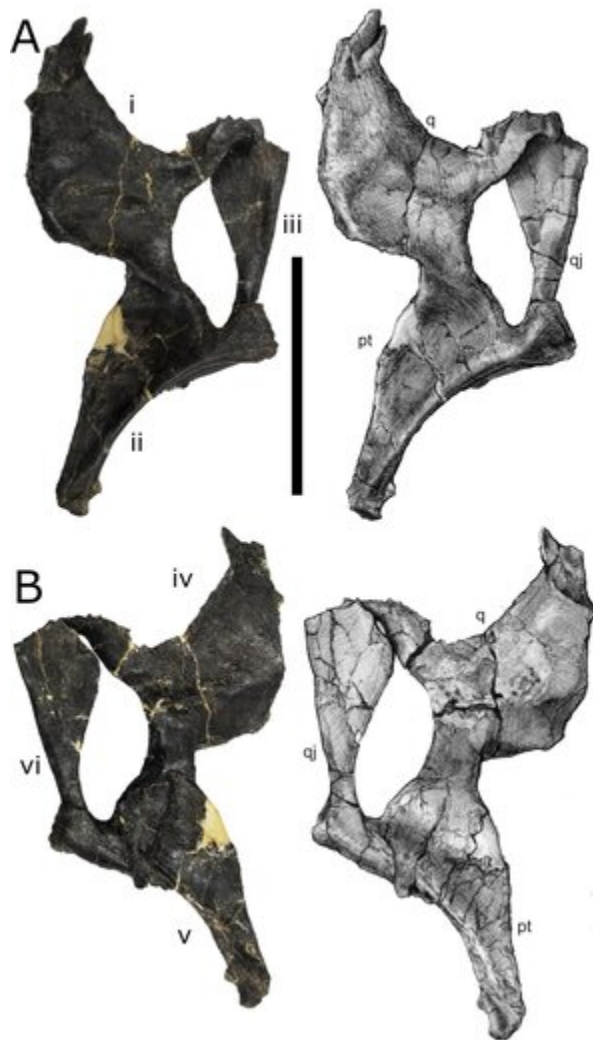
FIGURE 5. Left pterygoid (i, iv), quadrate (ii, v), and quadratojugal (iii, vi) in A) dorsal and B) ventral views. Scale bar equals 10 cm. Artwork by Ryan Steiskal. Abb: pt, pterygoid; q, quadrate; qj, quadratojugal.

reconstructed compared to the original specimen (Figure 8A-J). Reconstruction was done by one of the authors (MC) who has first-hand knowledge of the original material, type, and distribution of modifications. The basioccipital/basisphenoid complex did not undergo reconstruction. Only the region where nerves leaving the braincase (inside the orbit region) was modified as this area was crushed slightly dorsal ventrally.

The posterior face of the paroccipital process of TATE-099 is smooth and flat with a vertically expanded distal terminus. The supratemporal fenestra of TATE-099 is present with a maximum diameter of 1.2 times larger than the foramen magnum (Mannion et al., 2012). The anterodorsal margin of the supraoccipital is internally concave and

associated with a ventrally extending channel on the internal face. The dorsal extension of the supraoccipital is high and vaulted with sinuous dorsolateral edges, and the sagittal nuchal crest is broad but weakly developed. The crista prootica of TATE-099 laterally protrudes like other diplodocids but does not extend into the dorsolateral processes like in dicraeosaurids.

The articular surface of the occipital condyle of TATE-099 continuously grades into the condylar neck (Tschopp et al., 2015) with a broad basioccipital contribution to the occipital condylar neck (Harris and Dodson, 2004). Furthermore, the distance from the base of the occipital condyle to the base of the basal tubera is elongated with a flat region in between and a depression present between the foramen magnum and the basal tubera.

The basal tubera of TATE-099 itself is globular in shape, has a breadth that is 1.75 times the width of the occipital condyle, and is distinct from the basipterygoid. The posterior face of the basal tubera is flat with a continuous posteroventral face, has parallel long axes, and a concave anterior edge. In posterior view, the basal tubera faces straight ventrally, forming a horizontal line, and possesses a foramen notch that separates the two tubera. In ventral view, the posterior margin of the basitubera is approximately one condylar length anterior to the anterior margin of the occipital condyle.

Bakker (1998) suggested the position of the basitubera in *Apatosaurus ajax* was 'just forward of the occipital condyle' based on Berman and McIntosh (1978, which actually is describing CM 11162 and referred to *A. louisae,* not *A. ajax)* and 'far posterior to the position seen in' *Brontosaurus excelsus* (i.e., TATE-099 as assigned by Bakker, 1998). The reasoning for the assignment of TATE-099 to *B. excelsus* by Bakker (1998) is not explicitly stated using diagnostic skeletal apomorphies or formally cited. Considering there is not a skull associated with the holotype of *B. excelsus* (YPM 1980), no peer-reviewed publication of the proposed *B. excelsus* material from Nail Quarry, and no formal diagnosis of the few cervical vertebrae (unavailable for study) originally articulated with TATE-099, we consider this assignment to be unsupported. Furthermore, the position of the basitubera relative to the occipital condyle in *A. louisae* (CM 11162; Berman and McIntosh, 1978) is more anterior than suggested by Bakker (1998), and is consistent with morphology of TATE-099 (Figure S13).

The basipterygoid processes of TATE-099 are widely diverging (> 60º) and are oriented less than
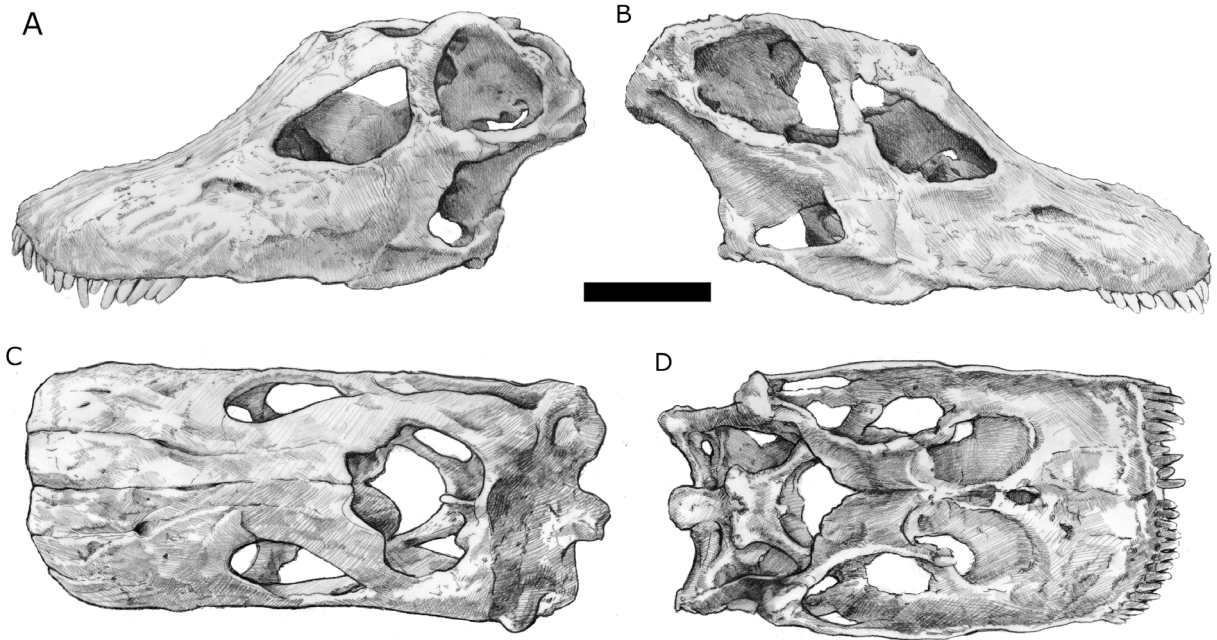
FIGURE 6. Reconstruction of the skull of TATE-099 in A) left lateral view, B) right lateral view, C) dorsal view, and D) ventral view. Scale bar equals 10 cm. Artwork by Ryan Steiskal.

75º to the skull roof (McIntosh, 1990), and lacks the basisphenoid/basipterygoid recess; both characters are apomorphic to the genus *Apatosaurus*. The ratio of length:basal transverse diameter of the basipterygoid processes is less than 4 (Wilson, 2002). The proximal-most portions of the basiptery-

goid processes are oriented similar to the central portion of the shaft. In anterior view, the distal ends of the processes are straight and lack the distal expansion observed in *Losillosaurus giganteus* (MCNV Lo-1 to 26) (Tschopp et al., 2015). Finally, the area between the basipterygoid processes and

FIGURE 7. Left (A) and right (B) ectopterygoid right and left lateral views (C, D). Scale bar equals 10 cm. Artwork by Ryan Steiskal.

FIGURE 8. Reconstructed cast and 3D model of the braincase of TATE-099 in dorsal view (A, B), ventral view (C, D), posterior view (E, F), right lateral view (G, H), and left lateral view (I, J). Scale bar equals 10 cm. Abb: bo, basoccipital; bpr, basipterygoid process; bs, basisphenoid; bt, basal tuber; cpr, crista prootica; eo, exoccipital-opithsotic; f, frontal; fm, foramen magnum; p, parietal; pas, parasphenoid; pft, posttemporal fenestra; po, postorbital; popr, paroccipital process; so, supraoccipital; snc, sagittal nuchal crest; stf, supratemporal fenestra.

the parasphenoid rostrum is mildly concave in shape, forming a subtriangular region.

Lower Jaw

The right dentary is preserved and possesses 11 alveolar positions. It measures 95 mm in length, 20 mm in thickness, and 90 mm in height. The dentary is oblong or rectangular in cross-sectional shape, and the anteroventral margin of the dentary is gently rounded (Tschopp et al., 2015; Whitlock and Harris, 2010). The dentary of TATE-099 lacks the tuberosity on the labial surface near the dentary symphysis that is present in the genera *Suuwassea* and *Dicraeosaurus* (Sereno et al., 2007; Tschopp et al., 2015; Whitlock and Harris, 2010). The right surangular and angular of TATE-099 is partially preserved, representing the posterior-most 170 mm of the complex, and measures 50 mm tall (Figure 9A-B).

Dentition

While no erupted, functional teeth of TATE-099 were available for description, CT imaging, segmentation, and 3D printing revealed long, narrow-crowned unerupted teeth in the alveoli that are typical of diplodocoids (Figures 10, 11); the crowns lack marginal denticles, the cross-sectional shape of tooth crowns at midcrown is cylindrical, and the crowns lack longitudinal grooves on the lingual aspect. The SI values (i.e., slenderness ratio of the crown length to the crown breadth (Upchurch, 1995) of the premaxilla, maxilla, and dentary of TATE-099 average 4.58, which is within the SI range of both *Apatosaurus* and *Dicraeosaurus* (Chure et al., 2010).

The shape of tooth row in occlusal view is anterolateral, and the corner of tooth row displaced labially, and the length of tooth rows is restricted anterior to antorbital fenestra. The orientation of tooth crowns is aligned along the jaw axis and the crowns are oriented anteriorly, and the crowns do not overlap, though the (Tschopp et al., 2015).

The number of unerupted crowns in the alveoli of the premaxilla, maxilla, and dentary vary considerably (Table 1); the premaxilla possesses 5-8 unerupted crowns in each alveolus, the maxillary alveoli each contain 3-5 crowns, and each alveolus of the dentary possesses 1-3 crowns. Measurements of the unerupted teeth are provided in Supplementary Tables S1-S4.

PHYLOGENETIC ANALYSIS

Phylogenetic Methods

TATE-099 is a relatively complete skull of an adult diplodocid sauropod. The specimen was reported to belong to *Brontosaurus excelsus* by Bakker (1998), with no evidence or justification for this taxonomic placement (see above). The intent of our phylogenetic analysis is to determine the most likely taxonomic placement of TATE-099 within Diplodocoidea using the Tschopp and others (2015) specimen-level matrix and Whitlock and Wilson's (2020) alpha-level matrix. Considering our inability to score TATE-099's postcranial material for inclusion in this study, we chose to test the phylogenetic position in both matrices, in part to compare results of a specimen-based matrix with a higher number of OTUs with representative cranial material (Tschopp et al., 2015) relative to a matrix with fewer skull-bearing alpha-level diplodocid OTUs (Whitlock and Wilson, 2020). The addition of TATE-099 into these data matrices (Supplementary Figures S14 and S15) is not likely to change the hypothesized tree topology presented in each respective study, however, the use of two different matrices may provide more robust support for the taxonomic identity of TATE-099 or highlight limitations in our understanding of diplodocoid cranial evolution. See Tschopp et al. (2015) for a complete list of OTUs and specimen catalog numbers used in the analysis and Supplementary Table S5 for taxa discussed in text; similarly, see Whitlock and Wilson (2020) for a complete list of OTUs.

Although we would prefer to score all of the collected elements assignable to theTATE-099 specimen, as mentioned above many of the original pieces including the braincase and at least six anteriormost cervicals remain either 'lost' (C1-2) or unavailable for study (i.e., C5-6?: thought to be unprepared in a field jacket at the Paleon Museum; C3-4: unprepared in field jacket at the Tate Geological Museum). Fortunately, the braincase—with minor but obvious reconstruction (alterations were performed by one of us [MC])—is represented by a high-fidelity resin replica curated alongside the remaining original material. We recognize that the use of replicas for phylogenetic analyses is not ideal, but first-hand knowledge of reconstruction enables us to confidently exclude any modified morphology from the analyses. Using the Tschopp and others (2015) matrix we were only able to score 38 characters when only original material was considered, however, an additional 53 characters were gained through the inclusion of the
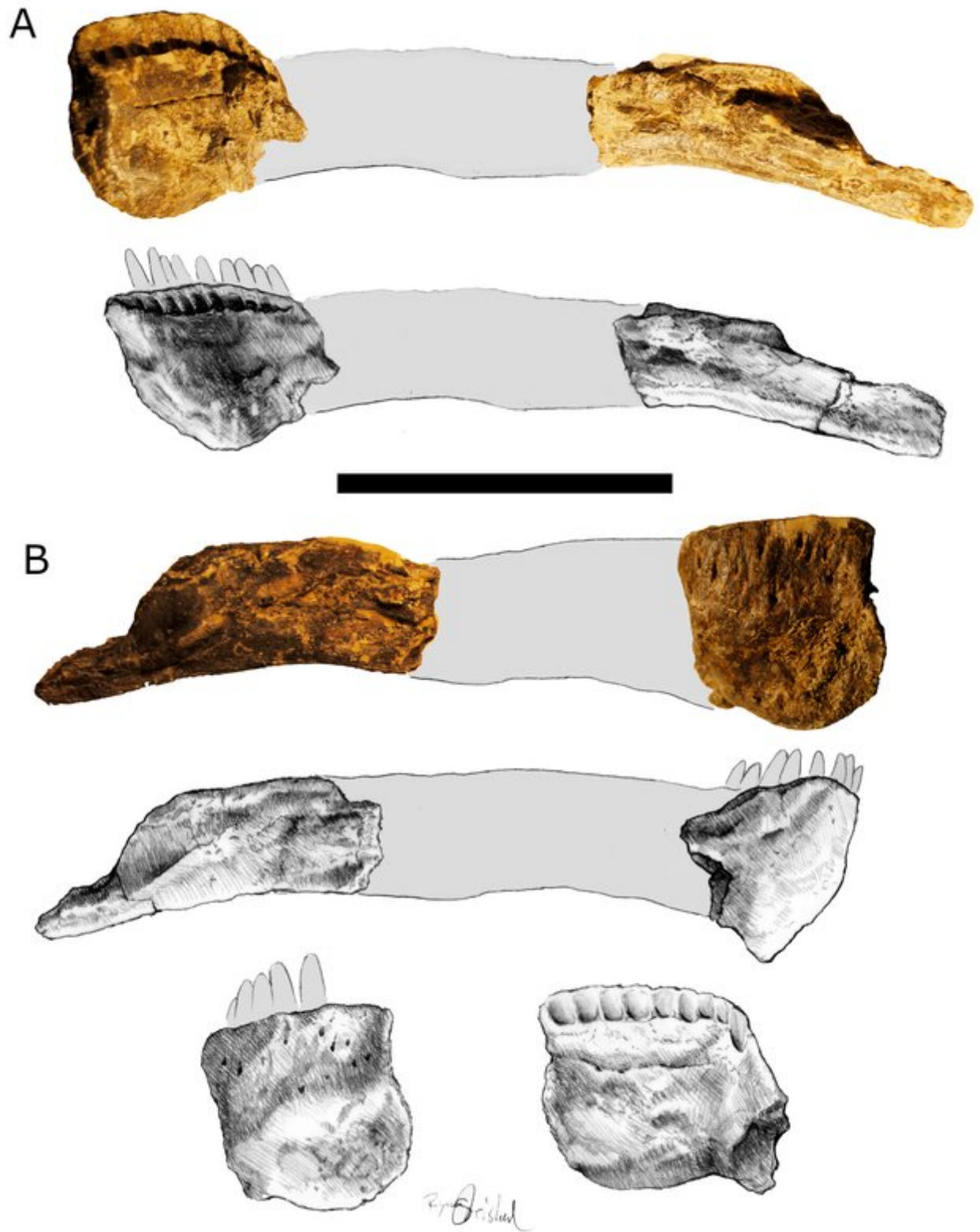
FIGURE 9. Right dentarty and surangular in A) left lateral view, and B) right lateral view. Scale bar equals 10 cm. Artwork by Ryan Steiskal.
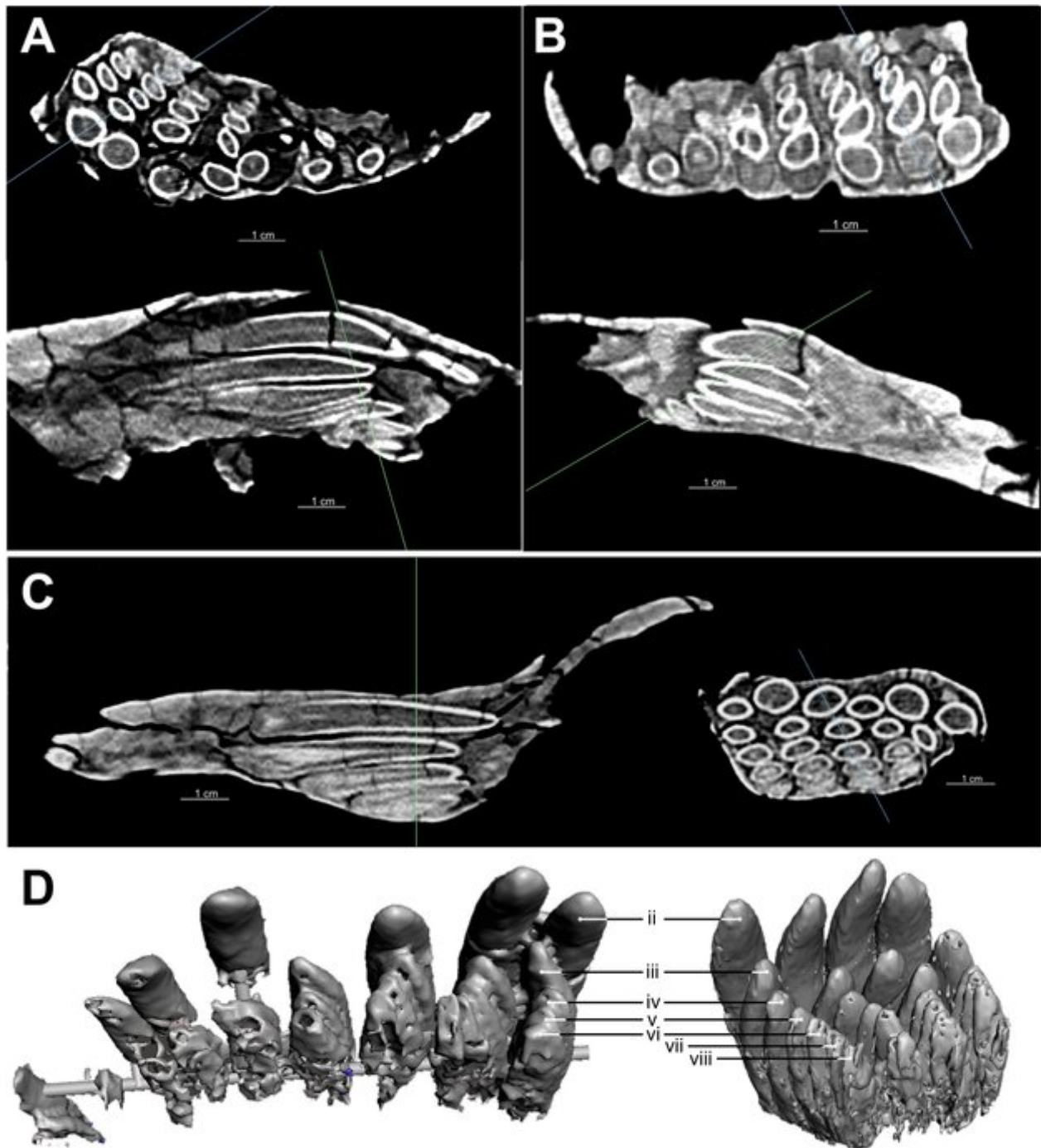
FIGURE 10. Computed tomography of the right and left maxillae (A-B, respectively) are displayed in coronal (upper) and sagittal (lower) cross sections; the left premaxilla (C) is shown in sagittal (left) and coronal (right) cross sections. The unerupted teeth (ii=first unerupted tooth) of the maxilla (D; left) and premaxilla (D; right) were segmented for 3D rapid prototyping. Note: proceeding caudally, the number of unerupted teeth in the maxilla declines from 5 (ii-vi) to 2 (ii-iii).
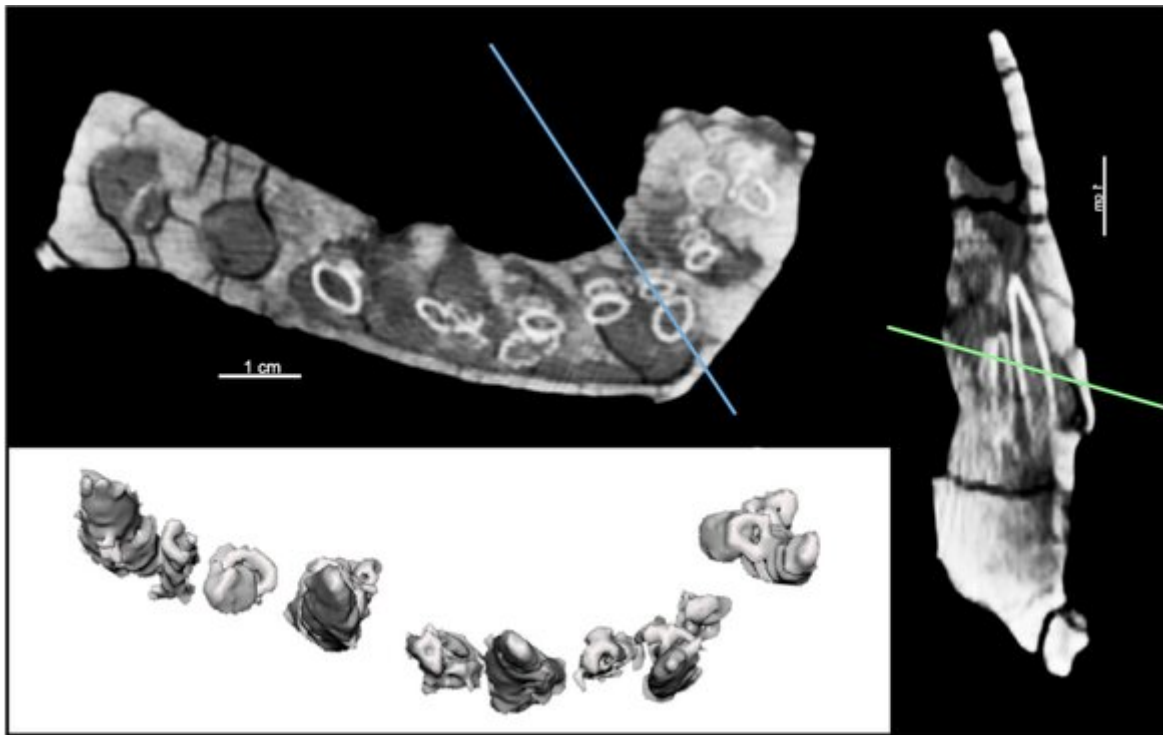
FIGURE 11. Computed tomography of the right dentary is displayed in coronal (left) and sagittal (right cross section, illustrating the presence of 1-2 unerupted teeth per alveolar position. The unerupted teeth were segmented for 3D rapid prototyping (lower left).

TABLE 1. Comparisons of Dental Complexes Among Neosauropods.

Genus	Specimen	Premaxilla		Maxilla		Dentary		Disparity		Reference
		Alveolar Positions	Replacement Teeth Per Alveolus	Alveolar Positions	Replacement Teeth Per Alveolus	Alveolar Positions	Replacement Teeth Per Alveolus	Dentary-to-Premaxilla	Dentary-to-Maxilla	
Apatosaurus	TATE-099	4	7-5	10	5-3	10	2-1			This study
	MWC-8430	4	7-4	-	-	-	-	0.29	0.4	McHugh (2018)
	MWC-6002	-	-	10	7-2	-	-			McHugh (2018)
Diplodocus	YPM 4677	4	5-3	11-9	5 (+)	-	-	-	-	D'Emic et al. (2013)
Dicraeosaurus	MB.R.2337-2339	4	5-4	-	-	-	-			Schwarz et al. (2015)
	MB.R.2336	-	-	12 (+)	4-1	-	-	0.6	0.75	Schwarz et al. (2015)
	MB.R.2371	-	-	-	-	16	3-1			Schwarz et al. (2015)
Camarasaurus	UMNH 5527	4	3-1	10-9	-	13	-	-	-	D'Emic et al. (2013)
Brachiosaurus	USNM 5730	4	2	13	1	14	1	0.5	1	D'Emic et al. (2019)
Nigersaurus	GDF512	4	10	24 (+)	10	34	10-8	1	1	Sereno & Wilson (2005)

- = unavailable for study

replica-based braincase. Analyses were conducted with all scorable characters including those attained from the replica-based braincase (i.e., n=91 out of 477, Tschopp et al., 2015; n=65 out of 203, Whitlock and Wilson, 2020).

The matrices were analyzed using TNT 1.5 (Goloboff and Catalano, 2016). After loading the data "Max Trees" under "Memory" in settings" was set to 99999. A "New Technology search" with "Sect.Search," "Ratchet," "Drift," and "Tree fusing" selected was performed as a "Driven search" to "Find min. length" 15 times and "Check level every" 3 hits. A strict consensus of all MPTs was done for each analysis; Trees>Consensus with "Strict (=Nelson) using "all trees" and "all taxa" selected. Bremer support was generated using the script "hold n*1000; sub n; bbreak=tbr;" where 'n' is repeated from 1 to 8), then "bsupport;" to generate a final supported tree. Bootstrap analyses were run with only the strict consensus tree in RAM and "Analyze>Resampling with Bootstrap, 'standard', and 'absolute frequencies' selected using 1000 replicates and a cutoff using 'groups from trees'.

Phylogenetic Results and Discussion

The addition of TATE-099 to the data matrix of Tschopp and others (2015) resulted in 47 MPTs with a minimum length of 1983, while the addition of TATE-099 to the Whitlock and Wilson (2020) matrix resulted in 23 MPTs with a minimum length of 360. Under the Tschopp and others (2015) analysis a strict consensus of all MPTs resulted in a significant polytomy with 51 nodes collapsed: CI= 0.17, RI=0.27 (Figure 12). However, the strict consensus maintains a sister relationship between *(Apatosaurus ajax* [YPM 1860] + TATE-099) and the polytomy *(A. laticollis* [YPM 1861] + *A. louisae* type + LACM 52844 + CM 3378). When the analysis was run with all braincase (i.e., replica-derived scores) removed, TATE-099 collapsed into a massive polytomy. Although the use of replicas for assigning character states is often eschewed, we believe these data are critically informative in this case and suggest that the phylogenetic hypotheses generated with their inclusion are valid.

As an additional test, we used the alpha-level OTU matrix of Whitlock and Wilson (2015) to further interrogate the phylogenetic position of TATE-099. A strict consensus of 23 MPTs maintained a similar topology to Whitlock and Wilson's findings with the exception of diplodocid OTUs in which 9 nodes collapsed into an unresolved polytomy with the inclusion of TATE-099; CI=0.57, RI=0.75 (Figure 13). Considering the paucity of diplodocid cra-
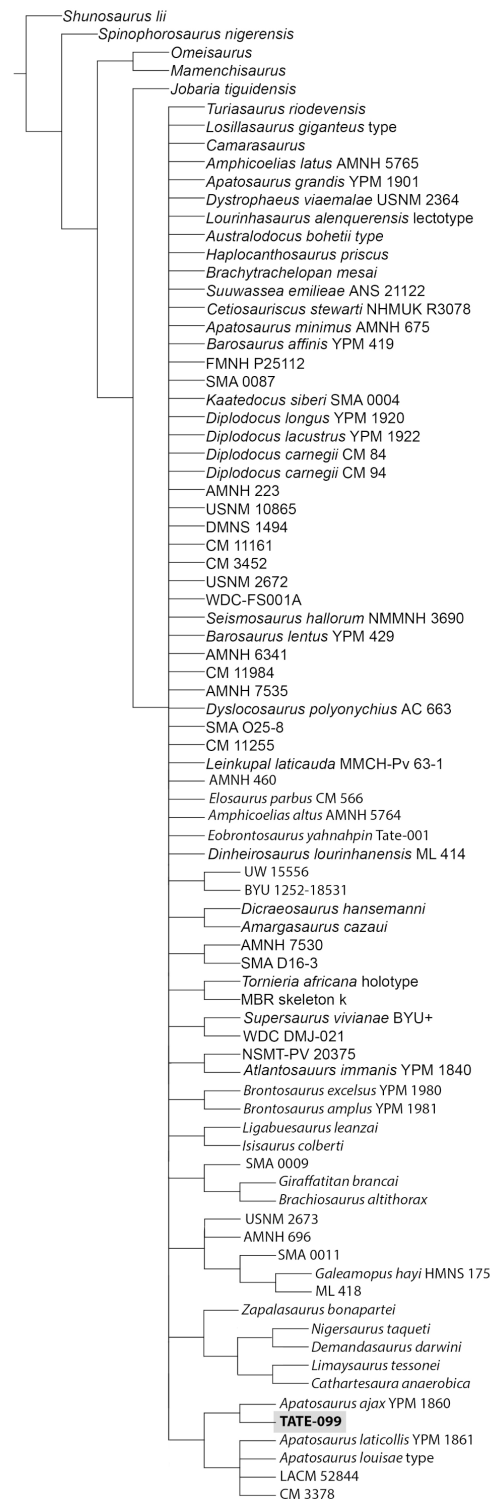

FIGURE 12. Strict consensus of 47 MPTs demonstrating the relative position of TATE-099 using the matrix of Tschopp and others (2015).

```
┌─ Omeisaurus
├─ Jobaria tiguidensis
│  Camarasaurus
│  ┌─ Australodocus bohetii
│  ├─ Giraffatitan brancai
│  Haplocanthosaurus priscus
│  ┌─ Zapalasaurus bonapartei
│  ├─ Limaysaurus tessoni
│  ├─ Histriasaurus boscarolli
│  ├─ Comahuesaurus windhauseni
│  ├─ Cathartesaura anaerobica
│  ├─ Amazonsaurus maranhensis
│  │  ┌─ Nigersaurus taqueti
│  │  ├─ Tataouinea hannibalis
│  │  ├─ Rebbachisaurus garasbae
│  │  └─ Demandasaurus darwini
│  TATE-099
│  Galeamopus pabsti
│  Apatosaurus louisae
│  Diplodocus carnegii
│  Tornieria africana
│  Supersaurus vivianae
│  Leinkupal laticauda
│  Dinheirosaurus lourinhaensis
│  Barasaurus lentus
│  ┌─ Kaatedocus siberi
│  ├─ Smitanosaurus agilis
│  │  ┌─ Bajadasaurus pronuspinax
│  │  ├─ MOR 592
│  │  Lingwulong shenqi
│  │  Suuwassea emilieae
│  │  Amargatitanis macni
│  │  Pilmatueia faundezi
│  │  ┌─ Dicraeosaurus hansemanni
│  │  ├─ Brachytrachelopan mesai
│  │  └─ Amargasaurus cazaui
```
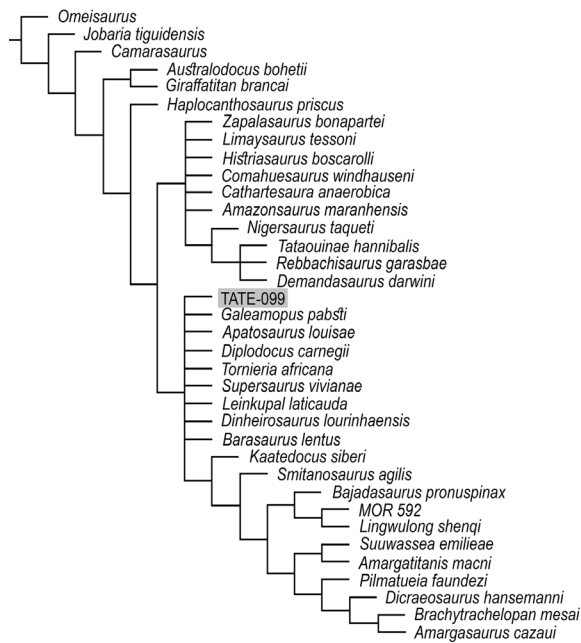
FIGURE 13. Strict consensus of 23 MPTs demonstrating the relative position of TATE-099 using the matrix of Whitlock and Wilson (2020).

nial material (i.e., four OTUs lacking any cranial material out of eight diplodocid OTUs analyzed) the collapse of this clade with the addition of a cranial specimen that lacks any postcranial data is not too surprising since *Diplodocus, Apatosaurus,* and TATE-099 had identical scorings, save for the distribution of missing characters, demonstrating that postcranial characters are what distinguish these two taxa in this analysis. Bootstrap values and Bremer support further highlight the reliance on postcranial characters to distinguish diplodocid OTUs (see Supplementary Figure S16.

Although the Whitlock and Wilson (2020) analysis was less phylogenetically informative than the Tschopp and others (2015) in the absence of postcranial characters (and thus overlap with the majority of known apatosaurine taxa) the nesting of TATE-099 within *Apatosaurus* in the strict consensus generated from the specimen-based analysis of Tschopp and others (2015) supports an assignment to *Apatosarus* sp.

It has been previously noted that some diplocines (i.e., *G. ['D'] hayi*) exhibit similarities to *Apatosaurus* in the skull, some apendicular, and caudal elements (McIntosh (1990); several analyses have demonstrated that *G. hayi* is consistently nested well within Diplodocinae (e.g., Tschopp et al., 2015; Whitlock and Wilson, 2020). The lack of unambigu-

ous cranial synapomorphies for either Apatosaurinae or Diplodocinae underscore the difficulty in determining TATE-099's position. Once specimens become available (or prepared), the inclusion of the TATE-099 anterior cervicals and (potentially) additional braincase characters into future analyses will aid in refining our current hypothesis. TATE-099's positions with and without the replica-based braincase characters in the Tschopp and others (2015) matrix also highlights the overall similarities of facial elements between known apatosaurine and diplodicine crania (i.e., table 4 of Tschopp et al., 2015).

DISCUSSION

Tooth Replacement in Neosauropoda

Among neosauropods, tooth replacement in the premaxillae, maxillae, and/or dentaries have been described in a variety of taxa, including the flagellicaudatan genera *Dicraeosaurus, Diplodocus,* and *Apatosaurus*, the macronarian genera *Brachiosaurus* and *Camarasaurus*, and the rebbachisaurid genus *Nigersaurus* (Table 1) (D'Emic et al., 2013, 2019; McHugh, 2018; Schwarz et al., 2015; Sereno and Wilson, 2005). Of these taxa, macronarians are measurably disparate from those of the clades Flagellicaudata (including TATE-099) and Rebbachisauridae in tooth volume, shape, replacement rate, as well as fewer numbers of replacement teeth (D'Emic et al., 2013, 2019). Although the maximum number of replacement teeth found in *Nigersaurus* is comparable with that observed in TATE-099, the teeth in *Nigersaurus* are smaller than those in the other examined diplodocid taxa, and *Nigersaurus* lacks alveolar septae, making the assignment of tooth replacement tows to individual erupted positions difficult (Sereno and Wilson, 2005).

Within Flagellicaudata the number, morphology, and general distribution of replacement teeth observed in the premaxilla and maxilla of TATE-099 are consistent with those described in isolated *Apatosaurus* sp. maxilla (MWC 6002) and premaxilla (MWC 8430) fragments from the Mygatt-Moore Quarry in the Morrison Formation (Brushy Basin Member) of western Colorado (McHugh, 2018). The Mygatt-Moore Quarry specimens are referred to the genus *Apatosaurus*, which we also assign to TATE-099 in this study. The premaxillae of both specimens show a maximum of seven replacement teeth, while the maxillae show similar numbers of replacement teeth, with the Colorado specimen preserving a higher number of maximum replace-

ment teeth (Table 1). As in MWC 8430, the lingually-directed inflection of the apical tooth crown in the premaxilla of TATE-099 is identifiable at position iv of the replacement row (= position v of McHugh, 2018) in the most mesial alveolar positions. The maxilla of TATE-099 shows some slight variation from the Mygatt-Moore specimen (MWC 6002), with a maximum of only five replacement teeth compared to seven in MWC 6002.

The tooth bearing elements of *Apatosaurus* (including TATE-099) exceed both *Diplodocus* and *Dicraeosaurus* in the maximum number of replacement teeth found in the premaxillae (7 teeth) and maxillae (5-7 teeth), while the dentary of TATE-099 shows the same number of replacement teeth as in *Dicraeosaurus* (D'Emic et al., 2019; Schwarz et al., 2015). This suggests a conservation of evolutionary changes to the dentition of the mandible compared to the disparity seen in the upper jaw. Even the dentary of the more distantly related genus *Brachiosaurus* (D'Emic et al., 2019) shows similar numbers of replacement teeth to those described here. This disparity may shed light on future studies of sauropod feeding biomechanics. Barrett and Upchurch (1995) proposed the use of the lower jaw in grasping, while the main tearing of the foliage was placed on the teeth in the upper jaw as the head pulled down and back. Although the propalinal motion required of the lower jaw in this biomechanical model has been shown to not be present in *Diplodocus* (Whitlock, 2017), the low disparity found in the replacement teeth in the dentaries of sauropods supports a low-impact use of the mandibular teeth in food acquisition. McHugh (2018) hypothesized that the higher number of replacement teeth observed in upper jaw elements of *Apatosaurus* over its contemporary *Diplodocus* was evidence of ecological niche partitioning, with *Apatosaurus* generally feeding on tougher vegetation than *Diplodocus*. We find no evidence to falsify that hypothesis; however, the low sample size of this comparative study, unfortunately, cannot distinguish between that scenario, individual variation, and regional ecophenotypic adaptations to differing plant diversity and availability.

Mechanism of Tooth Replacement

The erupted tooth row is not currently with the TATE-099 specimen and unavailable for study. However, photographs and cast replicas of the tooth row as it was originally found were available for this study (Figure 14A-C). The occlusal margin of the erupted tooth row shows distinct variation in the distribution of wear facets, with unworn teeth interspersed among worn tooth crowns. This variable crown height is mimicked in the preserved replacement teeth of the premaxilla and maxilla (Figure 14D, Table 1). Variation in crown height within the jaws creates the variation of wear facets and this appears to be shared in other diplodocid genera, including *Galemopus* and *Diplodocus* (figure 3 of Tschopp et al., 2015).

The mechanism for achieving this pattern is a unique process of tooth replacement among saurian reptiles. Unlike other thecodont reptiles, where teeth are individually replaced by resorbing the existing root of the erupted tooth and erupting within the same alveolus (Romer, 1956), CT data from the maxilla and premaxilla of TATE-099 show that the teeth in the first replacement tooth row are enlarged prior to eruption as an entire row, rather than individually, and the height of crowns varies among the row (Figure 14D, Table 1). This replacement row of multiple teeth of varying crown height is hypothesized here to have erupted as a complete row into the jaw and replaced the existing row as a single unit, rather than individually as in other thecodont reptiles. This is contrary to what is seen in *Camarasaurus* where teeth are alternatively replaced along the row to achieve the alternating pattern of wear facets through basic thecodont replacement (Chatterjee and Zheng, 2005). This "row-set" of tooth complex replacement creates a newly erupted tooth row with an uneven occlusal margin that through feeding will create the dispersed pattern of wear facets seen in the erupted tooth rows of many diplodocid genera. We hypothesize that this pre-eruption enlargement of the first row of replacement teeth is not observed in MWC 8340 or MWC 6002, because the tooth replacement row was not at the same stage of the eruption cycle as TATE-099 at time of the animals' deaths. Row-set tooth replacement appears to be present within *Apatosaurus, Galemopus,* and *Diplodocus*, and is possibly present in all diplodocids. More taxa need to be examined to assess the phylogenetic extent of this mechanism, as enlargement of replacement teeth by row is not observed in CT data of rebbachisaurid or macronarian taxa (D'Emic et al., 2013, 2019; Schwarz et al., 2015; Sereno and Wilson, 2005).

CONCLUSION

The relatively complete skull TATE-099, from Morrison Formation of Como Bluff (WY), exhibits a basipterygoid process that diverges greater than 60º and lacks the basisphenoid - basipterygoid recess consistent with the genus *Apatosaurus*.
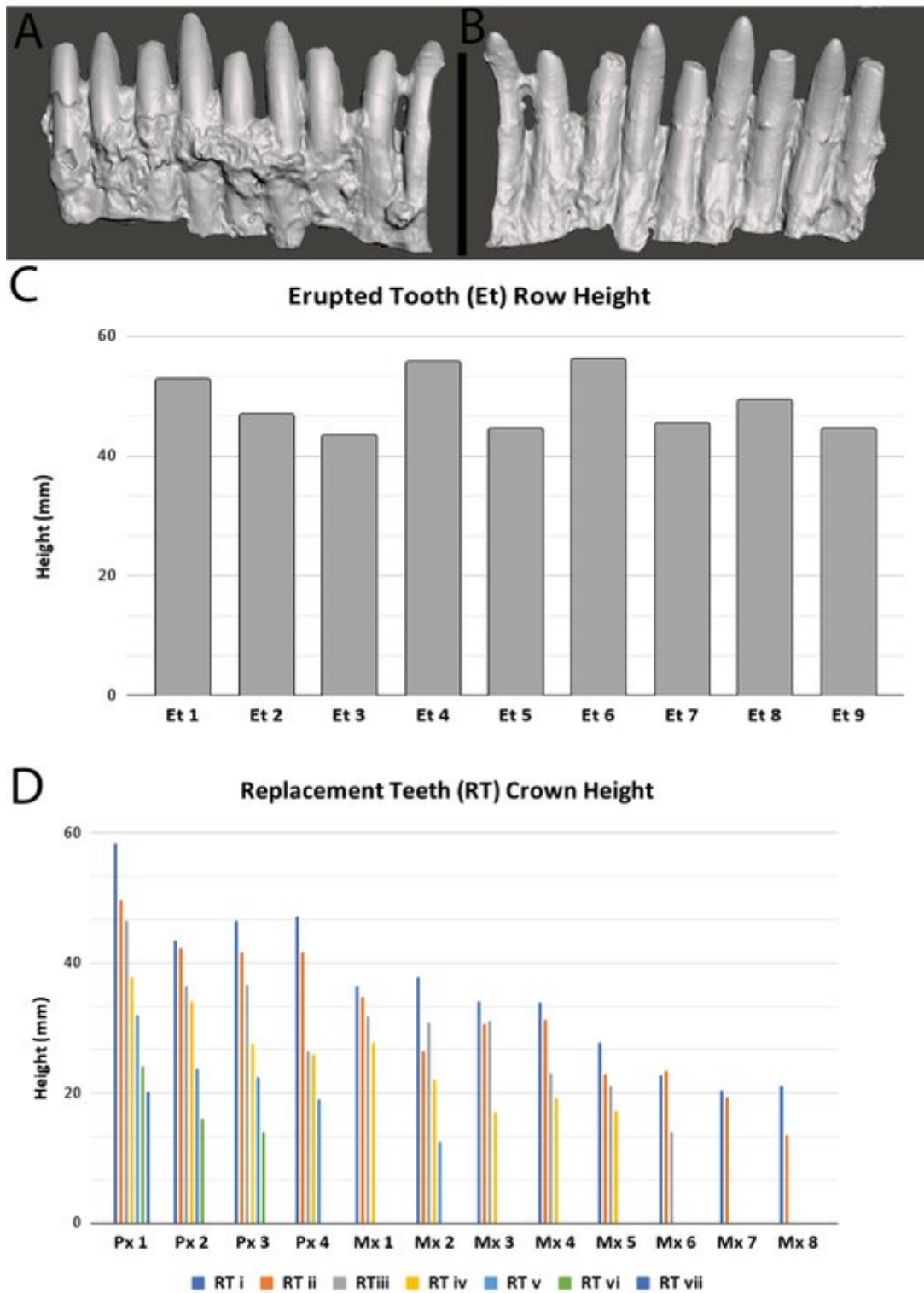
FIGURE 14. 3D model of a cast of the erupted tooth row of TATE-099 in (A) labial and (B) lingual views with crown heights (C) and comparative measurements of the unerupted replacement teeth (D). Scale bar equals 5 cm.

Although the braincase is currently missing, reproductions of the original make at least surficial scoring of phylogenetically important characters possible. With the inclusion of the replica-based braincase characters TATE-099 consistently is found sister to *Apatosaurus ajax*. However, when those characters are removed, analyses including only the remaining cranial characters more consistently find TATE-099 nested with *Galeamopus*, specifically with *G. pabsti,* highlighting a mosaic of shared facial characteristics amongst diplodocid sauropods. Whether these similarities are the result of non-selective pressures of diversification, biomechanical constraints, species recognition, or a combination thereof are still in need of further study.

Computed tomography scans made it possible to quantify replacement tooth count disparity between the dentary and both the premaxilla and maxilla of TATE-099. The premaxilla of TATE-099 has roughly triple the number of replacement teeth as the dentary, which is between 40-60 percent higher than in *Diplodocus*. The lower number of replacement teeth within the dentaries of TATE-099 and other diplodocoids may be indicative of lower biomechanical pressures on the mandible during food procurement (leaf raking) in these animals. The higher number of replacement teeth in the upper jaw of *Apatosaurus* relative to *Diplodocus* supports the ecological niche partitioning hypothesis within diplodocids, possibly pointing to *Apatosaurus'* preference for a food source with tougher vegetation. A larger taxonomic sample size is needed to more fully test this hypothesis. CT data also suggest a novel row-set tooth replacement mechanism, where entire rows of teeth are shed and replaced as a unit. This row-set tooth replacement appears to be shared across Diplodocidae.

Supplementary Files and CT Data

Supplementary files and raw CT data and of the right maxilla, premaxilla, and dentary of TATE-099 are available online at https://palaeo-electronica.org/content/2022/3653-apatosaurine-feeding-mechanism and also at https://figshare.com/account/home#/projects/131276.

REFERENCES

Allen, A. 1996. Morrison Formation stratigraphy between the classic Como Bluff and Thermopolis areas, Wyoming. Paleoenvironments of the Jurassic. Tate Museum Guidebook. Tate Museum, Casper, Wyoming, 1:19-28.

Bakker, R.T. 1996. The Real Jurassic Park: dinosaurs and habitats at Como Bluff, Wyoming. Museum of Northern Arizona Bulletin, 60:35-50.

Bakker, R.T., Wolberg, D.L., Stump, E., and Rosenberg, G.D. 1997. Raptor family values: allosaur parents brought giant carcasses into their lair to feed their young, p. 51-63. In Wolberg, D.L., Sump, E., and Rosenberg, G.D. (eds.), Dinofest International, Proceedings of a Symposium. Arizona State University, Tempe.

Bakker, R.T. 1998. Dinosaur mid-life crisis: The Jurassic-Cretaceous transition In Wyoming and Colorado. New Mexico Museum of Natural History and Science Bulletin, 14:67-76.

Bakker, R.T. and Bir, G. 2004. Dinosaur crime scene investigations: theropod behaviour at Como Bluff, Wyoming, and the evolution of birdness, p. 301-342. In Currie, P.J. (ed.), Feathered dragons: studies on the transition from dinosaurs to birds. Indiana University Press, Indiana.

Barrett, P.M. and Upchurch, P. 1995. Sauropod feeding mechanisms: their bearing on palaeoecology, p. 107-110. In Sun, A. and Wang, Y. (eds.), Sixth Symposium on Mesozoic Terrestrial Ecosystems and Biota. China Ocean Press, Beijing.

Berman, D.S. and McIntosh, J.S. 1978. Skull and relationships of the Upper Jurassic sauropod *Apatosaurus* (Reptilia, Saurischia). Bulletin of the Carnegie Museum of Natural History, 8:1-35.

Calvo, J.O. 1994. Jaw mechanics in sauropod dinosaurs. GAIA, 10:183-193.

Chatterjee, S. and Zheng, Z. 2005. Neuroanatomy and dentition of *Camarasaurus lentus*, p. 199-211. In Tidwell, V. and Carpenter, K. (eds.), Thunder-Lizards: The Sauropodomorph Dinosaurs. Indiana University Press, Bloomington.

Christian, A., Peng, G., Sekiya, T., Ye, Y., Wulf, M.G., and Steuer, T. 2013. Biomechanical reconstructions and selective advantages of neck poses and feeding strategies of Sauropods with the example of *Mamenchisaurus youngi*. PLoS ONE, 8(10): e71172. https://doi.org/10.1371/journal.pone.0071172.

Chure, D., Britt, B., Whitlock, J., and Wilson, J. 2010. First complete sauropod dinosaur skull from the Cretaceous of the Americas and the evolution of sauropod dentition. Naturwissenschaften, 97:379-391. https://doi.org/10.1007/s00114-010-0650-6

Connely, M.V. and Hawley, R. 1998. A proposed reconstruction of the jaw musculature and other soft cranial tissues of *Apatosaurus*. Journal of Vertebrate Paleontology, 18(Suppl. 3):35A.

Connely, M.V. 2002. Stratigraphy and Paleoecology of the Morrison Formation, Como Bluff, Wyoming. Unpublished Master Thesis. Utah State University. https://digitalcommons.usu.edu/etd/6736

Curry, K.A. 1999. Ontogenetic histology of *Apatosaurus* (Dinosauria: Sauropoda): new insights on growth rates and longevity. Journal of Vertebrate Paleontology, 19(4):654-665. https://doi.org/10.1080/02724634.1999.10011179.

D'Emic, M.D., Whitlock, J.A., Smith, K.M., Fisher, D.C., and Wilson, J.A. 2013. Evolution of high tooth replacement rates in sauropod dinosaurs. PLoS ONE, 8(7):e69235. https://doi.org/10.1371/journal.pone.0069235.

D'Emic, M.D., O'Connor, P.M., Pascucci, T.R., Gavras, J.N., Mardakhayava, E., and Lund, E.K. 2019. Evolution of high tooth replacement rates in theropod dinosaurs. PLoS ONE, 14(11): e0224734. https://doi.org/10.1371/journal.pone.0224734.

Dragonfly 2020.2 [Computer software]. Object Research Systems (ORS) Inc, Montreal, Canada, 2020; software available at http://www.theobjects.com/dragonfly.

Drumheller, S.K., McHugh, J.B., Kane, M., Riedel, A., and D'Amore, D.C. 2020. High frequencies of theropod bite marks provide evidence for feeding, scavenging, and possible cannibalism in a stressed Late Jurassic ecosystem. PLOS ONE, 15: e0233115. https://doi.org/10.1371/journal.pone.0233115.

Fiorillo, A.R. 1998. Dental microwear patterns of the sauropod dinosaurs *Camarasaurus* and *Diplodocus*: evidence for resource partitioning in the late Jurassic of North America. Historical Biology, 13:1-16. https://doi.org/10.1080/08912969809386568.

Foster, J.R. 2003. Paleoecological analysis of the vertebrate fauna of the Morrison Formation (Upper Jurassic), Rocky Mountain region, U.S.A. New Mexico Museum of Natural History and Science Bulletin, 23:1-95.

Foster, J.R. 2020. Jurassic West, 2nd Edition. Indiana University Press, Bloomington.

Foster, J.R. and Peterson, J.E. 2015. First report of *Apatosaurus* (Diplodocidae: Apatosaurinae) from the Cleveland-Lloyd Quarry in the Upper Jurassic Morrison Formation of Utah: Abundance, distribution, paleoecology, and taphonomy of an endemic North American sauropod clade. Palaeoworld, 25:431-443. https://doi.org/10.1016/j.palwor.2015.11.006.

Gee, C.T. 2011. Dietary options for the sauropod dinosaurs from an integrated botanical and paleobotanical perspective, p. 34-56. In Klein, N., Remes, K., Gee, C.T., and Sander, P.M. (eds.), Biology of the sauropod dinosaurs: Understanding the life of giants. Indiana University Press, Bloomington.

Goloboff, P.A. and Catalano, S.A. 2016. TNT version 1.5, including a full implementation of phylogenetic morphometrics. Cladistics, 32:221-238 https://doi.org/10.1111/cla.12160.

Harris, J.D. and Dodson, P. 2004. A new diplodocid sauropod dinosaur from the Upper Jurassic Morrison Formation of Montana, USA. Acta Palaeontologica Polonica, 49:197-210.

Huene, F.V. 1932. Die fossil Reptil-Ordnung Saurischia, ihre Entwicklung und Geschichte. Monographien zur Geologie und Palaeontologie, 4:1-361.

Hummel, J., Gee, C.T., Südekum, K.H., Sander, P.M., Nogge, G., and Clauss, M. 2008. In vitro digestibility of fern and gymnosperm foliage: implications for sauropod feeding ecology and diet selection. Proceedings of the Royal Society of London B: Biological Sciences, 275(1638):1015-1021. https://doi.org/10.1098/rspb.2007.1728.

Janensch, W. 1929. Die Wirbelsäule der Gattung *Dicraeosaurus*. Palaeontographica Supplement, 7:38-133.

Lehman, T.M. and Woodward, H.N. 2008. Modeling growth rates for sauropod dinosaurs. Paleobiology, 34:264-281. https://doi.org/10.1666/0094-8373(2008)034[0264:mgrfsd]2.0.co;2.

Maidment, S.C.R. and Muxworthy, A. 2019. A chronostratigraphic framework for the Upper Jurassic Morrison Formation, western U.S.A. Journal of Sedimentary Research, 89:1017-1038. https://doi.org/10.2110/jsr.2019.54.

Mannion, P.D., Upchurch, P., Mateus, O., Barnes, R.N., and Jones, M.E.H. 2012. New information on the anatomy and systematic position of *Dinheirosaurus lourinhanensis* (Sauropoda: Diplodocoidea) from the Late Jurassic of Portugal, with a review of European diplodocoids. Journal of Systematic Paleontology, 10:521-551. https://doi.org/10.1080/14772019.2011.595432.

Marsh, O.C. 1877. Notice of some new dinosaurian reptiles from the Jurassic Formation. American Journal of Science, 14:514-516.

Marsh, O.C. 1878. Principal characters of American Jurassic dinosaurs, Part I. American Journal of Science, 16:411-416.

Marsh, O.C. 1884. Principal characters of American Jurassic dinosaurs. Part VII. On the Diplodocidae, a new family of the Sauropoda. American Journal of Science, 27:160-168.

McMullen, S.K. 2017. Non-marine Stratigraphic paleobiology: a multi-scale examination. Unpublished PhD thesis, University of Wisconsin, Madison.

McHugh, J.B. 2018. Evidence for niche partitioning among ground-height browsing sauropods from the Upper Jurassic Morrison Formation of North America. Geology of the Intermountain West, 5:95-103. https://doi.org/10.31711/giw.v5.pp95-103.

McIntosh, J.S. 1990. Species determination in sauropod dinosaurs with tentative suggestions for their classification, p. 53-69. In Carpenter, K. and Currie, P.J. (eds.), Dinosaur systematics: perspectives and approaches. Cambridge University Press, New York.

Osborn, H.F. and Mook, C.C. 1921. *Camarasaurus*, *Amphicoelias*, and other sauropods of Cope. Memoirs of the American Museum of Natural History, New Series, 3:249-387.

Rees, P.M., Noto, C.R., Parrish, J.M., and Parrish, J.T. 2004. Late Jurassic climates, vegetation, and dinosaur distributions: Journal of Geology, 112:643-653. https://doi.org/10.1086/424577

Romer, A.S. 1956. The early evolution of land vertebrates. Proceedings of the American Philosophical Society, 100:157-167.

Salgado, L. and Calvo, J. 1992. Cranial osteology of *Amargasurus cazaui* Salgado & Bonaparte (Sauropoda, Dicraeosauridae) from the Neocomian of Patagonia. Ameghiniana, 29:337-346

Sander, P.M., Klein, N., Stein, K.O., and Wings, O. 2011. Sauropod bone histology and its implications for sauropod biology, p. 276-302. In Klein, N., Remes, K., Gee, C.T., and Sander, P.M. (eds.), Biology of the sauropod dinosaurs: Understanding the life of giants. Indiana University Press, Bloomington.

Schwarz, D., Kosch, J.C.D., Fritsch, G., and Hildebrandt, T. 2015. Dentition and tooth replacement of *Dicraeosaurus hansemanni* (Dinosauria, Sauropoda, Diplodocoidea) from the Tendaguru Formation of Tanzania. Journal of Vertebrate Paleontology, 35:e1008134. https://doi.org/10.1080/02724634.2015.1008134

Seeley, H.G. 1887. On the classification of the fossil animals commonly called Dinosauria. Proceedings of the Royal Society of London, 43:165-171.

Sereno, P.C. and Wilson, J.A. 2005. Structure and evolution of a sauropod tooth battery, p. 157-177. In Curry Rogers, K., and Wislon, J.A. (eds.), The Sauropods: Evolution and Paleobiology. University of California Press, Berkeley.

Sereno, P.C., Wilson, J.A., Witmer, L.M., Whitlock, J.A., Maga, A., Ide, O., and Rowe, T.A. 2007. Structural extremes in a Cretaceous dinosaur. PLoS ONE, 2:e1230 https://doi.org/10.1371/journal.pone.0001230.

Stevens, K.A. and Parrish, J.M. 2005. Digital reconstructions of sauropod dinosaurs and implications for feeding, p. 212-232. In Curry Rogers, K.A. and Wilson, J.A. (eds.), The Sauropods: Evolution and Paleobiology. University of California Press, Berkeley.

Tschopp, E. and Mateus, O. 2013. The skull and neck of a new flagellicaudatan sauropod from the Morrison Formation and its implication for the evolution and ontogeny of diplodocid dinosaurs. Journal of Systematic Palaeontology, 11:853-888. https://doi.org/10.1080/14772019.2012.746589.

Tschopp, E. and Mateus, O. 2017. Osteology of *Galeamopus pabsti* sp. nov. (Sauropoda: Diplodocidae), with implications for neurocentral closure timing, and the cervico-dorsal transition in diplodocids. PeerJ, 5:e3179 https://doi.org/10.7717/peerj.3179

Tschopp, E., Mateus, O., and Benson, R.B.J. 2015. A specimen-level phylogenetic analysis and taxonomic revision of Diplodocidae (Dinosauria, Sauropoda). PeerJ, 3:e857 https://doi.org/10.7717/peerj.857

Tschopp, E., Whitlock, J.A., Woodruff, D.C., Foster, J.R., Lei, R., and Giovanardi, S. 2022. The Morrison Formation Sauropod Consensus: A freely accessible online spreadsheet of collected sauropod specimens, their housing institutions, contents, references, localities, and other potentially useful information. Peer Community Journal, 2(e17). https://doi.org/10.24072/pcjournal.100

Tütken, T. 2011. The diet of sauropod dinosaurs – Implications from carbon isotope analysis of teeth, bones, and plants, p. 57-79. In Klein, N., Remes, K., Gee, C.T. and Sander, P.M. (eds.), Biology of the Sauropod Dinosaurs: Understanding the life of giants. Indiana University Press, Bloomington.

Upchurch, P. 1995. The evolutionary history of sauropod dinosaurs. Philosophical Transactions of the Royal Society of London Series B: Biological Sciences, 349:365-390. https://doi.org/10.1098/rstb.1995.0125.

Upchurch, P. 1999. The phylogenetic relationships of the Nemegtosauridae (Saurischia, Sauropoda) Journal of Vertebrate Paleontology, 19:106-125. https://doi.org/10.1080/02724634.1999.10011127.

Whitlock, J.A., Wilson, J.A., and Lamanna, M.C. 2010. Description of a nearly complete juvenile skull of *Diplodocus* (Sauropoda: Diplodocoidea) from the Late Jurassic of North America. Journal of Vertebrate Paleontology, 30:442-457. https://doi.org/10.1080/02724631003617647.

Whitlock, J.A. and Harris, J.D. 2010. The dentary of *Suuwassea emilieae* (Sauropoda: Diplodocoidea) Journal of Vertebrate Paleontology, 30:1637-1641. https://doi.org/10.1080/02724634.2010.501452.

Whitlock, J.A. 2011. Inferences of diplodocoid (Sauropoda: Dinosauria) feeding behavior from snout shape and microwear analyses: PLoS ONE, 6(4):e18304. https://doi.org/10.1371/journal.pone.0018304

Whitlock, J.A. 2017. Was *Diplodocus* (Diplodocoidea, Sauropoda) capable of propalinal jaw motion? Journal of Vertebrate Paleontology, 37(2):e1296457. https://doi.org/10.1080/02724634.2017.1296457

Whitlock, J., Trujillo, K., and Hanik, G. 2018. Assemblage-level structure in Morrison Formation dinosaurs, western interior, USA. Geology of the Intermountain West, 5:9-22. https://doi.org/10.31711/giw.v5.pp9-22

Wilson, J.A. 2002. Sauropod dinosaur phylogeny: critique and cladistic analysis. Zoological Journal of the Linnean Society, 136:215-275. https://doi.org/10.1046/j.1096-3642.2002.00029.x

Wilson, J.A. 2005. Overview of sauropod phylogeny and evolution, p. 15-49. In Curry Rogers, K.A. and Wilson, J.A. (eds.), The Sauropods: Evolution and Paleobiology. University of California Press, Berkeley.

SUPPLEMENTARY MATERIALS

The following Supplementary Materials are available at:
https://palaeo-electronica.org/content/2022/3653-apatosaurine-feeding-mechanism
and also https://figshare.com/account/home#/projects/131276.

Figure and Table Captions

FIGURE S1. STL model of the left premaxilla of TATE-099.
FIGURE S2. STL model of the right premaxilla of TATE-099.
FIGURE S3. STL model of the left maxilla of TATE-099.
FIGURE S4. STL model of the right maxilla of TATE-099.
FIGURE S5. STL model of the left pterygoid and quadrate of TATE-099.
FIGURE S6. STL model of the left quadratojugal of TATE-099.
FIGURE S7. STL model of the left palatine of TATE-099.
FIGURE S8. STL model of the left ectopterygoid of TATE-099.
FIGURE S9. STL model of the right ectopterygoid of TATE-099.
FIGURE S10. STL model of the right dentary of TATE-099.
FIGURE S11. STL model of the right surangular of TATE-099.
FIGURE S12. STL model of the braincase (cast) of TATE-099.
FIGURE S13. Comparison of the basioccipital-basisphenoid complex of TATE-099 to three other diplodoc-ids (modified after Tschopp et al., 2015).
FIGURE S14. Tschopp et al. 2015 matrix with TATE-099 with replica-based braincase.
FIGURE S15. Whitlock and Wilson, 2020 - matrix with characters of TATE-099 added.
FIGURE S16. Bremmer support and Bootstrap values.
TABLE S1. Replacement tooth measurements of the right premaxilla of TATE-099.
TABLE S2. Replacement tooth measurements of the right maxilla of TATE-099.
TABLE S3. Replacement tooth measurements of the right dentary of TATE-099.
TABLE S4. Measurements of the crown heights of the erupted maxillary teeth of TATE-099.
TABLE S5. Specimen numbers and taxa used for comparisons with TATE-099.

Dataset files

TATE-099 Right Dentary CT Data - Dataset
TATE-099 Right Maxilla CT Data - Dataset
TATE-099 Right Premaxilla CT Data - Dataset